Solar-Terrestrial Physics. 2026, vol. 12, iss.1, pp. 59–67. DOI: 10.12737/stp-121202608. © 2026
A.S. Nikitenko, O.M. Lebed, A.V. Larchenko, Yu.V. Fedorenko. Published by INFRA-M Academic Publishing House

DOI: 10.12737/stp-121202608
EDN: PLBXQK

Received May 07, 2025
Accepted September 01, 2025

ANALYZING EVENTS OF SIMULTANEOUS GROUND-BASED REGISTRATION OF AURORAL HISS BURSTS AND RIOMETRIC ABSORPTION INCREASE

A.S. Nikitenko
Polar Geophysical Institute KSC RAS,
Apatity, Russia, alex.nikitenko91@gmail.com

O.M. Lebed
Polar Geophysical Institute KSC RAS,
Apatity, Russia, olga.m.lebed@gmail.com

A.V. Larchenko
Polar Geophysical Institute KSC RAS,
Apatity, Russia, alexey.larchenko@gmail.com

Yu.V. Fedorenko
Polar Geophysical Institute KSC RAS,
Apatity, Russia, yury.fedorenko@gmail.com

Abstract. The paper presents the results of the analysis of nine simultaneous ground-based detection events of auroral hiss bursts at the Lovozero Observatory and cosmic radio noise absorption (riometric absorption) at the Lovozero and Tumanny observatories located on the Kola Peninsula. We have estimated the position of the area of increased absorption, using the results of riometric observations at these observatories and images from all-sky cameras in the Lovozero Observatory and nearby locations. The position of the area "illuminated" by auroral hisses was determined by measuring the azimuthal angle of the Poynting vector and the polarization of the magnetic field of the hisses. It has been found that for each event considered the area of illumination and the area of increased riometric absorption are located at different latitudes. This may explain the cases of simultaneous ground-based observations of the two phenomena in question, although auroral hisses usually disappear with a significant increase in riometric absorption.

Keywords: auroral hiss, ionosphere, cosmic noise absorption.

INTRODUCTION

Generation of electromagnetic emission in Earth's magnetosphere is a typical manifestation of space weather. An example of such emission is auroral hisses — electromagnetic noise waves [Sazhin et al., 1993; LaBelle, Treumann, 2002]. Hisses are recorded in the frequency range from a few to several hundred kilohertz and are characterized by the absence of a pronounced time-frequency structure in spectrograms. The maximum hiss intensity is at very low frequencies 8–10 kHz (VLF, 3–30 kHz).

Auroral hisses propagate in plasma in a whistler mode. They are generated by the interaction between <10 keV electron flux and plasma, which causes the Cherenkov instability [Sazhin et al., 1993; Makita, 1979; Maggs, 1976]. Auroral hisses are an important indicator of wave–particle interactions in the magnetosphere, which are essential to the dynamics of near-Earth plasma [Makita, 1979; Spasojevic, 2016; Kleimenova et al., 2019]. According to [Kleimenova et al., 2019], auroral hisses are most intensively generated in the equatorial part of the auroral oval during the magnetospheric substorm growth phase. However, upon the onset of the auroral breakup, hiss bursts cease abruptly, which, according to Kleimenova et al. [2019], is due to a sudden increase in VLF wave absorption in the ionosphere.

Auroral hisses are emissions most frequently detected near the Earth surface at high latitudes. They propagate to Earth due to scattering by small-scale electron density irregularities in the ionosphere [Sonwalkar, Harikumar, 2000].

Spatial distribution of the hiss field near the Earth surface features a well-defined locality [Harang, Larsen, 1965; Jørgensen, 1966; Srivastava, 1976; Makita, 1979]. Observations at the observatories Tromsø (corrected geomagnetic latitude Φ~70°) and Kiruna (Φ~65°), spaced ~250 km apart, revealed significant differences between intensities of hiss bursts at these points [Harang, Larsen, 1965]. The concentration of auroral hiss intensity in a local region near the Earth surface was also found in [Jørgensen, 1966; Srivastava, 1976] from ground-based observations at 13 stations. In our previous works [Nikitenko et al., 2022, 2023], it has been established that the illumination area (the term we introduced to denote the reception zone of hisses near the Earth surface) can be both small (<400 km) and extended in longitude.

Observations show that the location of the illumination area is related to the location of the auroral hisses accompanying auroras [Makita, 1979], but the illumination area is shifted relative to the auroral zone to lower latitudes. This is attributed to the peculiarities of radiation propagation outside plasma irregularities stretched along geomagnetic field lines (so-called ducts) [Helliwell, 1965]. This effect was further confirmed by Ozaki et al. [2008] when analyzing ground-based observations of auroral hisses at spaced points in Antarctica.

Auroral hisses are recorded much less frequently near the Earth surface than at satellite altitudes [Gurnett, 1966; Hughes et al., 1971]. One of the primary causes of this may be the increased absorption of VLF waves in the ionosphere. In our study [Nikitenko et al., 2025], we have quantitatively assessed the effect of riometric ab-

sorption (absorption of cosmic radio noise) on the conditions of penetration of hisses into the Earth surface, using a model of their propagation [Lebed et al., 2019]. The results have shown that when passing through the undisturbed ionosphere the hiss power near the Earth surface is by 13 dB lower than at 800 km. An increase in the riometric absorption to 0.6 dB leads to additional attenuation of the signal by 45–50 dB, as a result of which the power of the bursts becomes comparable to the intrinsic noise level of the Earth–ionosphere waveguide. With the absorption level of 2.2 dB, the signal is attenuated by 80 dB, which, in fact, eliminates the possibility of detecting this radiation near the Earth surface.

Although auroral hisses do not reach the Earth surface at riometric absorption above 0.6 dB, a correlation is experimentally observed between their bursts and changes in absorption [Harang, Larsen, 1965; Jørgensen, 1966]. As shown in [Jørgensen, 1966], this correlation is typical of low absorption levels, whereas with a significant increase in absorption, hisses cannot be further observed.

During observations from September 1 to December 31, 2023 at the Lovozero and Tumanny observatories (Kola Peninsula), there were nine events of simultaneous detection of auroral hiss bursts and riometric absorption enhancement. In this paper, in order to explain the phenomenon we present the results of comparison between locations of the absorption region and the auroral hiss illumination area as observed at these stations.

The paper is structured as follows: Section 1 describes the equipment, noise suppression and data processing methods; Section 2 defines and interprets the events of simultaneous detection of hisses and riometric absorption increase; Section 3 analyzes the spatial discrepancy between zones of absorption and detection of hisses, explained by scattering mechanisms in the inclined geomagnetic structure; in Conclusion, we summarize the key results of the study, formulate the main conclusions on the mechanisms of auroral hiss propagation and their relationship with riometric absorption, and outline directions for future research.

1. GROUND-BASED OBSERVATIONS AND DATA ANALYSIS

The paper uses observation data on the electromagnetic field of auroral hisses from the Lovozero Observatory (LOZ, geographic coordinates 67.97° N, 35.02° E), on the absorption level of cosmic radio noise from the Lovozero and Tumanny (TUM, 69.07° N, 35.73° E) observatories, as well as all-sky camera data from the Verkhnetulomsky Obseratory (VTU, 68.36° N, 31.47° E) and Lovozero station. Figure 1 shows the location of the observation points.

Equipment

To detect the electromagnetic field of auroral hisses, a receiver is employed which measures two horizontal magnetic field components and the vertical electric field component [Pil'gaev et al., 2021]. These three components are used to determine the form and orientation of the magnetic field polarization ellipse, as well as the magnitude and direction of the Poynting vector necessary for analyzing the

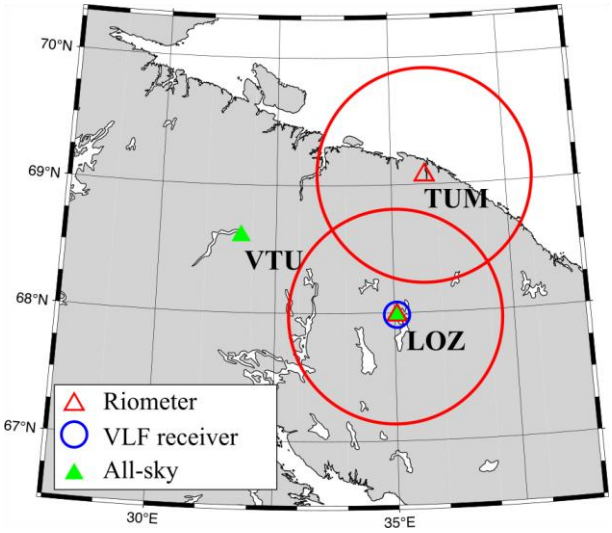

Figure 1. Location of observation points. Red circles indicate riometer antennas' fields of view

location of the auroral hiss illumination area [Tsuruda, Ikeda, 1979, Rytov, 1966]. Measurements are carried out with definite reference to UT [Pil'gaev et al., 2021] in a VLF frequency range from 300 Hz to 15 kHz.

Measurements of the absorption level of cosmic radio noise are made with a riometer designed and manufactured at the Polar Geophysical Institute. The riometer detects cosmic radio noise absorption in a narrow range of angles relative to the zenith. A signal is received by a 2×2 phased array antenna consisting of three-element Yagi-Uda antennas, which at a level of –3 dB has a narrow radiation pattern of ~44°, thereby reducing noise from ground sources by 15–20 dB compared to an antenna with a wide radiation pattern. Cosmic radio noise absorption is recorded in the frequency band from 37.5 to 39.5 MHz, which makes it possible to suppress narrowband noise by identifying and excluding it from processing. The riometric absorption values have been obtained by subtracting the diurnal cosmic noise absorption curve from data under quiet geomagnetic conditions.

The developed riometers have a high spatial resolution. Figure 1 presents the riometer antennas' fields of view marked with red circles centered at the LOZ and TUM points. If we conceive a radio signal source as a hemisphere with a constant brightness of each point, we can identify a region within which one or another part of the power received by the riometer antenna from the entire luminous hemisphere is concentrated. We set the reception zone at an altitude of 90 km, where maximum absorption of cosmic radio noise takes place [Hargreaves, 1969]. In this case, the reception zone is an area where the power received by an antenna is 90 % of the total received power, i.e. if an absorption of 3 dB occurs in the reception zone, but nothing changes outside it, the riometer will show an absorption of 2.7 dB.

Noise attenuation

Ground-based observations of the electromagnetic field in a frequency range below 15 kHz are extremely noisy with interference of various types, mainly with pulsed sferics — electromagnetic signals excited by a

lightning discharge. According to our observations, it can take to 30–40 % of the hourly observation interval to record sferics. Interference of another type is harmonics of narrowband signals from a 50 Hz network and the transmitter ZEVS. To analyze auroral hisses, we suppress these signals in recordings of field components.

The sferic detection algorithm is based on the analysis of the envelope of the horizontal magnetic field component H_τ [Manninen et al., 2021]. Pulses are detected by identifying signals whose amplitude exceeds a given threshold level H_{tr}. Pulse boundaries are determined from the points of change of the sign of the derivative of the envelope. If the envelope values at the points, where the boundaries are defined, exceed the threshold, the fragment is regarded as a sequence of pulses. In this case, the boundaries are iteratively expanded to the nearest points of crossing the threshold H_{tr}. Isolated pulses (or their sequences) are excluded from all three field components. The resulting gaps are filled in through linear interpolation.

The threshold level H_{tr} is set adaptively according to the formula $H_{tr}=2.45\sigma_{opt}$, where σ_{opt} is a 0.25 quantile of H_τ distribution, which allows powerful hiss bursts to remain unscathed. Quantiles are calculated at short time intervals of H_τ envelope splitting. Figure 2, *a*, *c* illustrates the time dependence of quantiles of the $p(H_\tau)$ distribution and the signal-to-noise ratio for quantiles of different orders, calculated for observations at LOZ on November 30, 2023 (17:06:40–17:18:20 UT). The signal was defined as an RMS deviation of the envelope between red dashed lines (see Figure 2, *c*); the noise, as an RMS deviation of the values to the left of the black dashed line. Analysis shows that hiss bursts are prominent at quantiles less than 0.5, and the optimal signal-to-noise ratio is achieved at 0.25 quantile. Figure 2, *b*, *d* displays spectrograms of the horizontal magnetic field component before and after sferic suppression, which demonstrate that the initial hiss burst was completely masked by sferics.

To suppress interference from the 50 Hz network and the ZEVS transmitter, harmonics within their band are cut out on the spectrum of field component recordings. The resulting segments are filled with complex white delta-correlated Gaussian noise whose covariance matrix [Rytov, 1966] corresponds to the average matrix calculated from spectra along edges of the scrap.

Estimated location of the auroral hiss illumination area

To determine the spatial location of the auroral hiss illumination area, two key parameters are analyzed: polarization and direction of radiation arrival.

Polarization of detected radiation is widely used to estimate the distance to the center of the illuminated area [Tsuruda et al., 1982; Machida and Tsuruda, 1984; Yearby, Smith, 1994; Titova et al., 2015; Manninen et al., 2018, 2021]. According to the theory of electromagnetic wave propagation, only waves with right circular polarization (relative to the direction of the geomagnetic field) can propagate in ionospheric plasma in the VLF band [Stix, 1992]. In a clockwise-polarized wave, the magnetic field vector rotates in a plane across the same direction of wave propagation as an electron propagates in the geomagnetic field [Stix, 1992]. Clockwise-polarized waves

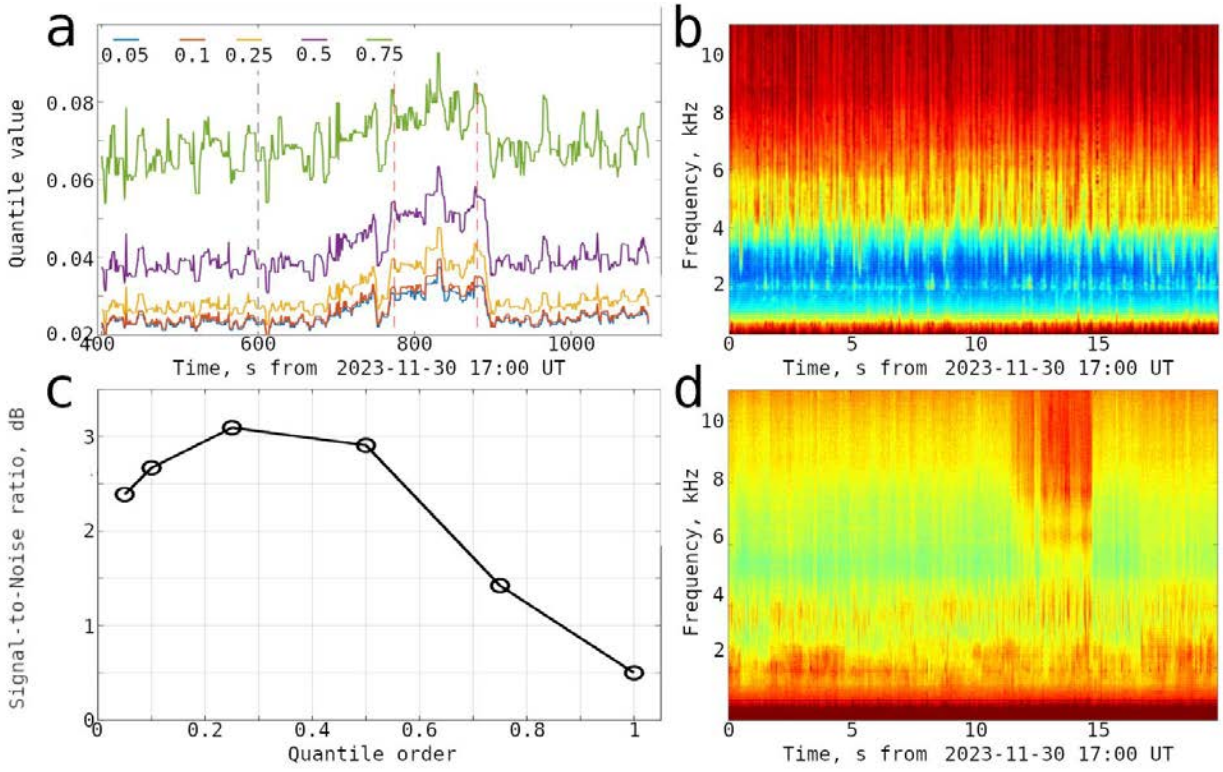

Figure 2. Time dependence of reciprocal distribution $p(H_\tau)$ (*a*), signal-to-noise ratio for quantiles of different orders (*c*), spectrograms of the horizontal magnetic field component before (*b*) and after (*d*) suppression of sferics, calculated for LOZ observations on November 30, 2023 at 17:00–17:20 UT

penetrate from the ionosphere into the Earth surface; therefore, radiation with right polarization is observed in the vicinity of the center of the illumination area [Nikitenko et al., 2022; Yearby, Smith 1994; Manninen et al., 2018, 2021]. Counterclockwise-polarized radiation is detected at a distance from the center of the illumination area due to the reflection of waves from the upper anisotropic wall of the Earth–ionosphere waveguide and the dominance of the reflected wave over the straight line [Xu et al., 2019; Nikitenko et al., 2022].

To quantify radiation polarization, we employ the circular polarization index P_c [Rytov, 1966], which takes values from –1 to 1: at $P_c>0$, wave polarization is clockwise; at $P_c<0$, counterclockwise; at $P_c=0$, linear. If $|P_c|=1$, polarization is circular.

To estimate the direction of wave arrival at an observation point, we use the back azimuth of Poynting vector — the angle the vector opposite to the Poynting vector makes with a direction to the north [Nikitenko et al., 2022; Manninen et al., 2021].

2. ANALYSIS RESULTS

From September 1 to December 31, 2023, we recorded nine simultaneous events of auroral hiss bursts and riometric absorption enhancement (Figure 3): December 10, 18:00–18:20 UT (1); December 5, 19:50–20:10 UT (2); December 13, 22:40–23:00 UT (3); November 22, 18:10–18:30 UT (4); December 5, 19:10–19:30 UT (5); October 26, 19:10–19:30 UT (6); November 9, 17:10–17:30 UT (7); December 21, 00:00–00:20 UT (8); November 22, 15:00–15:20 UT (9). For these events, Figure 3 exhibits LOZ and TUM spectrograms of the horizontal magnetic field component with riometric absorption variations. In these cases, the riometric absorption level varies from 0.25 to 1–1.2 dB, at which ground-based detection of hisses is impossible [Nikitenko et al., 2025].

In events 1–5, 7, and 8, absorption bursts accompanying hiss bursts are recorded only at TUM (see Figure 3), whereas at LOZ there are almost no even weak absorption bursts. In event 9, an absorption increase is detected at LOZ in the absence of any absorption variations at TUM. In event 6, a hiss burst is observed at equal riometric absorption values at LOZ and TUM.

In events 1–5, 7, and 8, the equatorial boundary of the patch in the ionosphere appears to be located at a latitude higher than LOZ. Since LOZ and TUM fields of view partially overlap (see Figure 1), when this boundary is closer to LOZ, an absorption enhancement should also be recorded at this observatory. Since this does not happen, we assume that the equatorial boundary of the patch is located in the vicinity of TUM. In event 6, the same absorption level is recorded at both points, i.e. at this time the patch center is between LOZ and TUM.

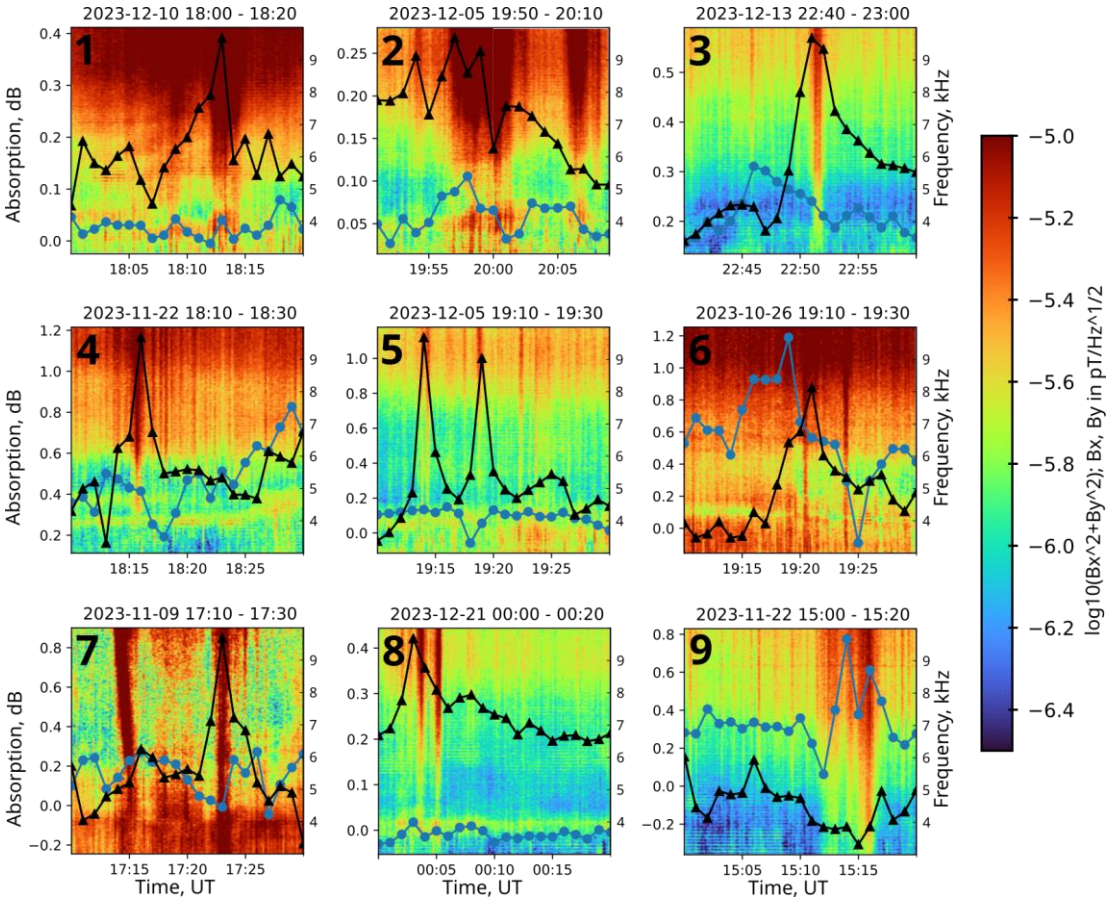

Figure 3. Spectrograms of the horizontal magnetic field component for simultaneous detection of auroral hisses and riometric absorption enhancement with superimposed riometric absorption variations at LOZ (blue curve) and TUM (black curve)

There are no absorption variations at TUM in event 9. At this moment, the polar boundary of the patch is located outside the boundary of the reception zone at TUM, closer to LOZ.

The assumptions about the location of the patch are confirmed by the location of auroras in the events considered. Figure 4 presents all-sky camera images from LOZ and VTU taken during maximum intensity of auroral hiss bursts for events 2–4, 5 (two bursts), and 7–9.

In event 9 (an increase in the absorption level only at LOZ), according to LOZ data, the arc is located somewhat south of this point (see Figure 4, *h*). Assuming that the size of the patch in latitude depends on the size of the auroral arc, we can suppose that the equatorial boundary of this region is 30–50 km south of LOZ.

In other events, auroral activity occurs north of LOZ (Figure 4, *a*–*g*). Note that in event 1 (December 10, 18:00–18:20 UT) favorable weather conditions made it possible to observe auroras at Kevo Observatory (Sweden, 69.76° N, 27.01° E), located ~400 km northwest of LOZ. According to the all-sky camera images (data not shown), auroral activity in this event was recorded at higher latitudes than the latitude of LOZ, with the equatorial boundary of the auroras located at least 100 km north of LOZ.

We have analyzed the features of variations in polarization and direction of arrival of auroral hiss bursts at LOZ in order to estimate the location of their illumination area. Figures 5 and 6 show the back azimuth of Poynting vector and the circular polarization index for the events of interest. According to Figure 5, it is only in event 8 (December 21, 00:00–00:20 UT) that auroral hisses arrive at the observation point from the west, i.e. the center of the illumination area is at the same latitude as LOZ. Judging by the variations in the direction of arrival at frequencies above 5 kHz, in events 1–7 and 9 auroral hisses arrive at the observation point from lower latitudes, mainly from the southwest or southeast. In events 1, 7, and 9, radiation of a different type, apparently coming from the north and northeast, is recorded at frequencies below ~5 kHz.

According to the results of the calculation of the circular polarization index, all auroral hiss bursts considered have clockwise polarization (see Figure 6). A clockwise almost circular polarization, when the P_c index takes values close to 1, is observed in event 7 (November 9, 17:10–17:30 UT), i.e. the center of the auroral hiss illumination area is quite close to LOZ. In other events, polarization is elliptical and the center of the illumination area is located at some distance from LOZ.

Thus, bursts at frequencies below ~5 kHz arriving at LOZ from the north and northeast have counterclockwise polarization in event 1, i.e. their illumination area is far from LOZ, and clockwise polarization close to circular in events 7, 9, i.e. their illumination area is close to LOZ.

3. DISCUSSION

According to the analysis results, an absorption region local in latitude is recorded in the events under study. In events 1–5, 7, the equatorial boundary of this region is located in the vicinity of TUM (see Figure 3); in event 6, the center of this region is between LOZ and TUM; in event 9, its polar boundary is 30–50 km south of LOZ.

The results of the analysis of the azimuth angles of auroral hiss arrival at the observation point and the polarization of their magnetic field show that in all the events considered the location of the absorption region does not coincide with the location of the auroral hiss illumination area. In event 8, the center of the auroral hiss illumination area is located at the LOZ latitude to the west of it. At the same time, according to observations of auroras at Kevo Observatory, the equatorial boundary of the patch is located at least 100 km north of LOZ. In all other events, the center of the auroral hiss illumination area is at lower latitudes than the equatorial boundary of the patch.

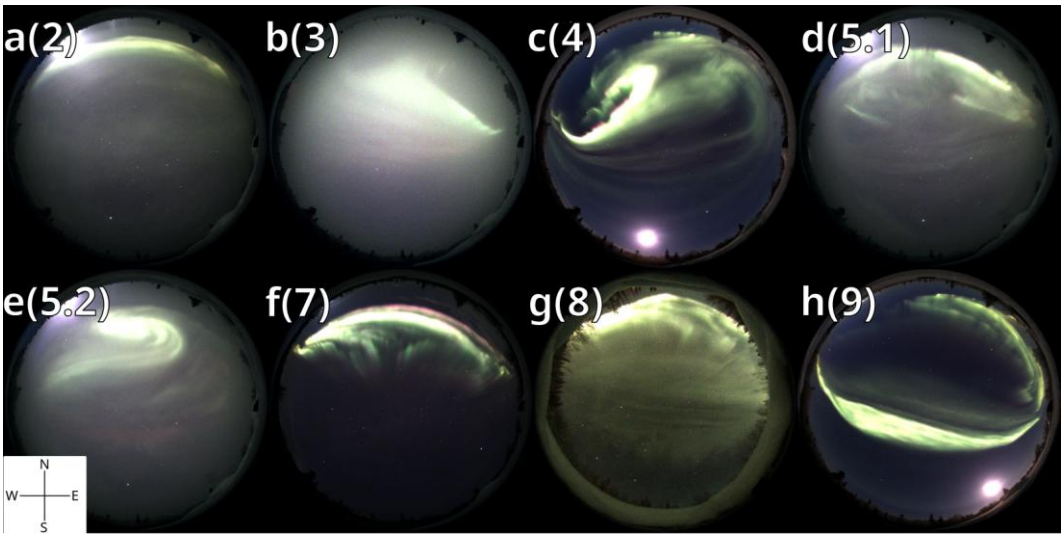

Figure 4. Images from all-sky cameras, installed in LOZ (*a*–*f*, *h*) and VTU (*g*), taken at ten second intervals corresponding to the maximum auroral hiss bursts for events 2–5, 7–9: December 5, 19:59:00–19:59:10 UT (*a*); December 13, 22:51:30–22:51:40 UT (*b*), November 22, 18:15:40–18:15:50 UT (*c*); December 5, 19:14:20–19:14:30 UT (*d*); December 5, 19:18:30–19:18:40 UT (*e*); November 9, 17:23:00–17:23:10 UT (*f*), December 21, 00:03:30–00:03:40 UT (*g*); November 22, 15:16:00–15:16:10 UT

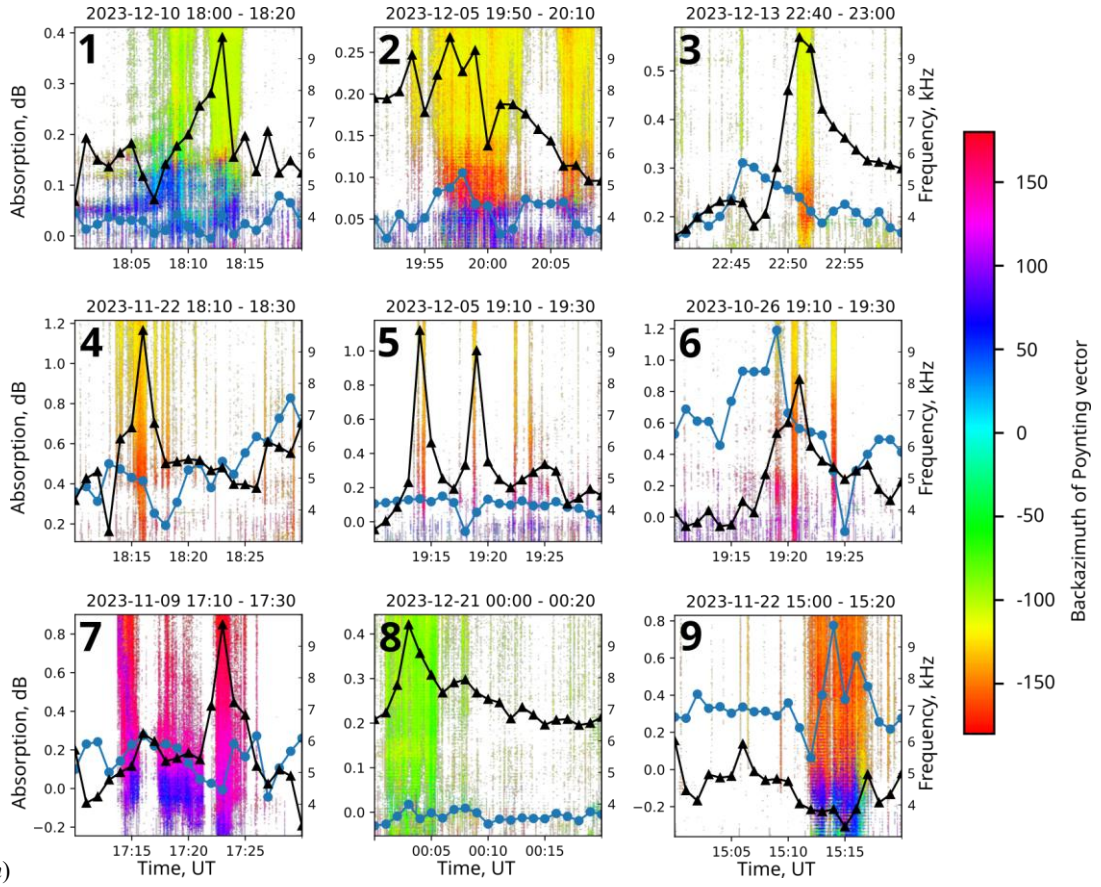

(*h*)

Figure 5. Back azimuth of Poynting vector for events 1–9 (see Figure 2)

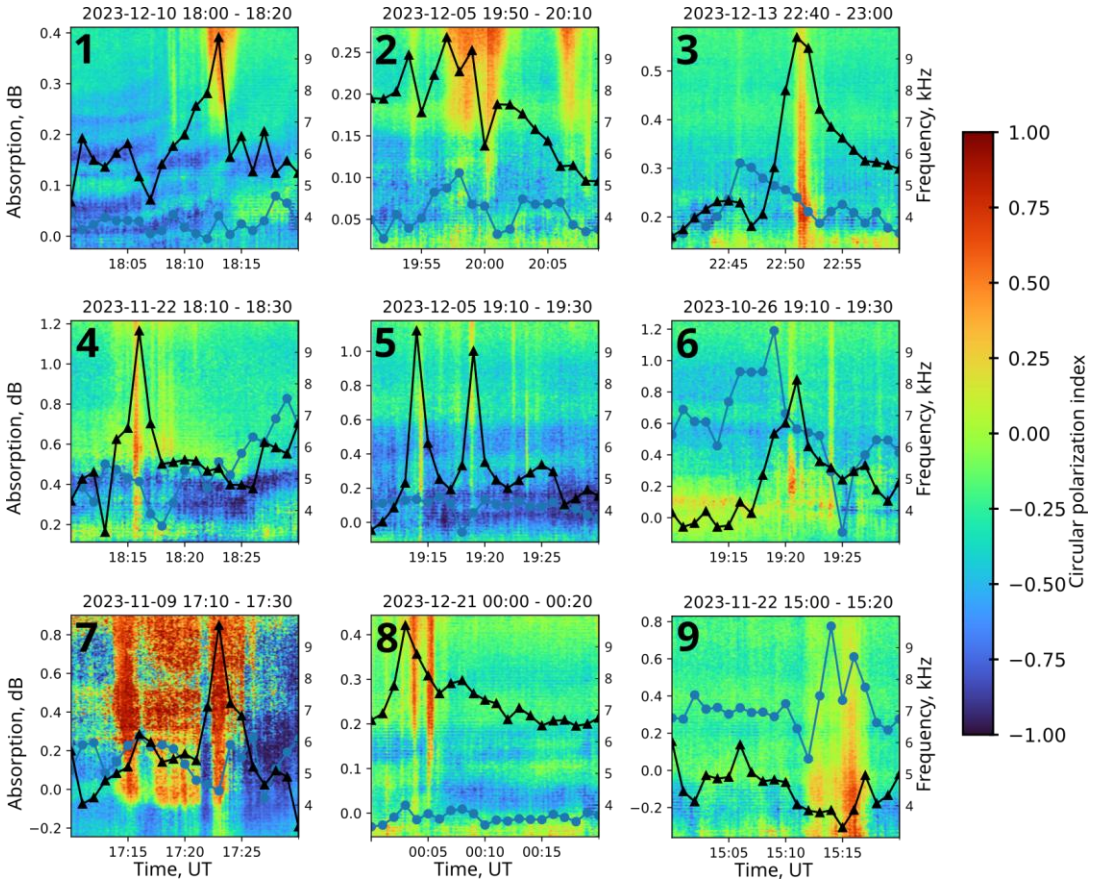

Figure 6. Circular polarization index for events 1–9 (see Figure 2)

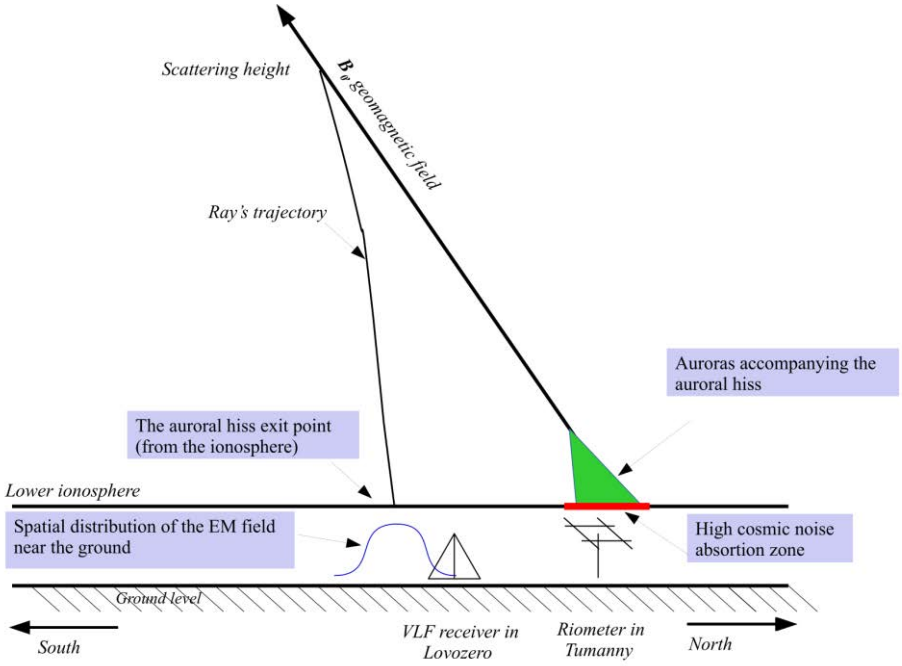

Figure 7. Adapted scheme of auroral hiss propagation to the Earth surface (proposed in [Makita, 1979; Ozaki et al., 2008])

Figure 7 presents an adapted scheme for auroral hiss propagation to the Earth surface, proposed in [Makita, 1979; Ozaki et al., 2008]. Auroral hisses are scattered by small-scale electron density irregularities in the upper ionosphere, where the refractive index $n \geq 5$. It follows from Snell's law [Stix, 1992] that only waves with wave normals close to the vertical can reach the Earth surface, where the refractive index is 1. Beams of energetic electrons, which excite hisses and cause an increase in cosmic radio noise absorption in the lower ionosphere, penetrate into the ionosphere, where they generate auroras, along geomagnetic field lines. Since scattering occurs quite high (800 km and above) [Sonwalkar, Harikumar, 2000; Nikitenko et al., 2023; Shklyar, Nagano, 1998; Kuzichev, 2012], due to geomagnetic field inclination the distance between the footpoint of the magnetic field line and the center of the illumination area can be as large as several hundred kilometers. Owing to this effect, auroral hisses will be recorded at lower latitudes than their accompanying auroras and hence the absorption region.

An additional argument in favor of the locality of the absorption region is observation of two spaced VLF emission bursts in events 1, 7, and 9. In events 7 and 9, the identical time-frequency structure of low-latitude and high-latitude bursts indicates their common nature associated with auroral hiss. In event 1, the low-frequency component (<5 kHz) of the second burst probably has a different origin.

In events 7 and 9, bursts with the direction of arrival from higher latitudes may result from the formation of two beams of quasi-electrostatic waves in the meridional plane, which excite auroral hisses [Nikitenko et al., 2023]. They can also arise from scattering by small-scale irregularities of a beam propagating to the pole from the field line on which the hisses were generated. Simultaneous detection of two auroral hiss illumination areas separated by latitude with increasing riometric absorption may suggest that the absorption region is local in latitude. Otherwise, a higher-latitude burst propagating to the Earth surface would not be recorded when entered the absorption region due to attenuation.

CONCLUSION

We have reported the results of the analysis of nine events of simultaneous detection of auroral hiss bursts and riometric absorption enhancement. In some events, the absorption level reached values at which, according to the results obtained in [Nikitenko et al., 2025], the hisses cannot arrive at the Earth surface due to attenuation in the lower ionosphere.

Comparing the location of the auroral hiss illumination area and the riometric absorption region as observed at the Lovozero and Tumanny observatories has revealed that the centers of the hiss illumination area are shifted relative to the riometric absorption region to lower latitudes. Optical observations made by all-sky cameras have confirmed the spatial separation of these regions. We have found that in the events of interest the region of auroras causing increases in riometric absorption is shifted to higher latitudes relative to the hiss illumination area.

The obtained results indicate that the beam of energetic electrons responsible for the generation of hisses and the appearance of auroras creates a bounded region of increased riometric absorption in the lower ionosphere. Due to the narrow propagation cone of waves with a frequency below 15 kHz, auroral hisses after scattering in the upper ionosphere by small-scale electron density irregularities reach the Earth surface at lower latitudes than those at which the absorption region is located [Makita, 1979; Ozaki et al., 2008].

The proposed mechanism explains the simultaneous detection of auroral hiss bursts and high riometric absorption levels (more than ~0.6 dB), which, according to model estimates, should completely suppress propagation of VLF emission to the Earth surface. This model can be verified through 3D modeling of VLF wave propagation, taking into account the real structure of the ionosphere, as well as joint analysis of satellite (in situ) and ground-based measurements for direct determination of scattering altitudes and location.

The work was financially supported by RSF Grant No. 24-27-20048 "Assessment of Ionospheric Conditions in the Arctic Zone from Results of Ground-Based Measurements of the Electromagnetic Field of Auroral Hisses in the Very Low Frequency Range and Riometric Absorption."

REFERENCES

Jørgensen T.S. Morphology of VLF hiss zones and their correlation with particle precipitation events. *J. Geophys. Res.* 1966, vol. 71, iss. 5, pp. 1367–1375. DOI: 10.1029/JZ071i005p01367.

Gurnett D.A. A satellite study of VLF hiss. *J. Geophys. Res*. 1966, vol. 71, pp. 5599–5615.

Harang L., Larsen R. Radio wave emissions in the VLF-band observed near the auroral zone. I. Occurrence of emissions during disturbances. *J. Atmos. Terr. Phys*. 1965, vol. 27, pp. 481–497. DOI: 10.1016/0021-9169(65)90013-9.

Hargreaves J.K. Auroral absorption of HF radio waves in the ionosphere: A review of results from the first decade of riometry. *Proc. IEEE.* 1969, vol. 57, pp. 1348–1373. DOI: 10.1109/PROC.1969.7275.

Helliwell R.A. *Whistler and Related Ionospheric Phenomena*. Stanford, Stanford Univ. Press, 1965, 349 p.

Hughes A.R.W., Kaiser T.R., Bullough K. The frequency of occurrence of VLF radio emissions at high latitudes. *Space Res.* 1971, vol. 11, pp. 1323–1330.

Kleimenova N.G., Manninen J., Gromova L.I., Gromov S.V., Turunen T. Bursts of auroral-hiss VLF emissions on the Earth's surface at *L*~5.5 and geomagnetic disturbances. *Geomagnetism and Aeronomy*. 2019, vol. 59, pp. 272–280. DOI: 10.1134/S0016793219030083.

Kuzichev I.V. On whistler mode wave scattering from density irregularities in the upper ionosphere. *J. Geophys. Res.: Space Phys*. 2012, vol. 117, iss. A6. DOI: 10.1029/2011JA017130.

LaBelle J., Treumann R.A. Auroral radio emissions. 1. Hisses, roars, and bursts. *Space Sci. Rev.* 2002, vol. 101, pp. 295–440. DOI: 10.1023/A:1020850022070.

Lebed' O.M., Fedorenko Y.V., Manninen J., Kleimenova N.G., Nikitenko A.S. Modeling of the auroral hiss propagation from the source region to the ground. *Geomagnetism and Aeronomy*. 2019, vol. 59, pp. 577–586. DOI: 10.1134/S0016793219050074.

Machida S., Tsuruda K. Intensity and polarization characteristics of whistlers deduced from multi-station observations. *J. Geophys. Res.: Space Phys*. 1984, vol. 89, iss. A3, pp. 1675–1682. DOI: 10.1029/JA089iA03p01675.

Maggs J.E. Coherent generation of VLF hiss. *J. Geophys. Res.* 1976, vol. 81, pp. 1707–1724. DOI: 10.1029/JA081i010p01707.

Makita K. VLF/LF hiss emissions associated with aurora. *Mem. Nat. Inst. Polar Res. Ser. A.* 1979, iss. 16, pp. 1–126.

Manninen J., Kleimenova N., Turunen T., Gromova L. New high-frequency (7–12 kHz) quasi-periodic VLF emissions observed on the ground at *L* ~5.5. *Ann. Geophys.* 2018, vol. 36, pp. 915–923. DOI: 10.5194/angeo-36-915-2018.

Manninen J., Kleimenova N., Turunen T., Nikitenko A., Gromova L., Fedorenko Y. New type of short high-frequency VLF patches ("VLF birds") above 4–5 kHz. *J. Geophys. Res.: Space Phys.* 2021, vol. 126, E2020JA028601. DOI: 10.1029/2020JA028601.

Nikitenko A.S., Manninen J., Fedorenko Y.V., Kleimenova N.G., Kuznetsova M.V., Larchenko A.V., et al. Spatial structure of the illuminated area of the auroral hiss based on ground-based observations at auroral latitudes. *Geomagnetism and Aeronomy*. 2022, vol. 62, pp. 209–216. DOI: 10.1134/S0016793222030124.

Nikitenko A.S., Fedorenko Y.V., Manninen J., Lebed O.M., Beketova E.B. Modeling the spatial structure of the auroral hiss and comparing results to observations. *Bull. Russ. Acad. Sci. Phys*. 2023, vol. 87, pp. 112–117. DOI: 10.3103/S1062873822700265.

Nikitenko A.S., Lebed O.M., Larchenko A.V., Fedorenko Yu.V. Analysis of the effect of cosmic noise absorption increase on propagation of auroral hiss to the ground. *Sol.-Terr. Phys*. 2025, vol. 11, iss. 1, pp. 63–69. DOI: 10.12737/stp-111202508.

Ozaki M., Yagitani S., Nagano I., Hata Y., Yamagishi H., Sato N., Kadokura A. Localization of VLF ionospheric exit point by comparison of multipoint ground-based observation with full-wave analysis. *Polar Sci.* 2008, vol. 2, iss. 4, pp. 237–249. DOI: 10.1016/j.polar.2008.09.001.

Pil'gaev S.V., Larchenko A.V., Fedorenko Y.V., Filatov M.V., Nikitenko A.S. A three-component very-low-frequency signal receiver with precision data synchronization with universal time. *Instruments and Experimental Techniques.* 2021, vol. 64, pp. 744–753. DOI: 10.1134/S0020441221040229.

Rytov S.M. *Vvedenie v statisticheskuyu radiofiziku* [Introduction to Statistical Radiophysics]. Moscow, Nauka Publ., 1966, 404 p. (In Russian).

Sazhin S.S., Bullough K., Hayakawa M. Auroral hiss: a review. *Planetary and Space Sci.* 1993, vol. 41, pp. 153–166. DOI: 10.1016/0032-0633(93)90045-4.

Shklyar D.R., Nagano I. On VLF wave scattering in plasma with density irregularities. *J. Geophys. Res.: Space Phys.* 1998, vol. 103, iss. A12, pp. 29515–29526. DOI: 10.1029/98JA02311.

Sonwalkar V.S., Harikumar J. An explanation of ground observations of auroral hiss: Role of density depletions and meter-scale irregularities. *J. Geophys. Res.: Space Phys.* 2000, vol. 105, iss. A8, pp. 18867–18883. DOI: 10.1029/1999JA00030.

Spasojevic M. Statistics of auroral hiss and relationship to auroral boundaries and upward current regions. *J. Geophys. Res.: Space Phys*. 2016, vol. 121, pp. 7547–7560. DOI: 10.1002/2016JA022851.

Srivastava R.N. VLF hiss, visual aurora and the geomagnetic activity. *Planetary and Space Sci*. 1976, vol. 24, pp. 375–379. DOI: 10.1016/0032-0633(76)90050-7.

Stix T. *Waves in Plasmas*. American Institute of Physics, 1992, 579 p.

Titova E.E., Kozelov B.V., Demekhov A.G., Manninen J., Santolik O., Kletzing C.A., Reeves G. Identification of the source of quasiperiodic VLF emissions using ground-based and Van Allen Probes satellite observations. *Geophys. Res. Lett.* 2015, vol. 42, pp. 6137–6145. DOI: 10.1002/2015GL064911.

Tsuruda K., Ikeda M. Comparison of three different types of VLF direction-finding techniques. *J. Geophys. Res.* 1979, vol. 84, iss. A9, pp. 5325–5332. DOI: 10.1029/JA084iA09p05325.

Tsuruda K., Machida S., Terasawa T., Nishida A., Maezawa K. High spatial attenuation of the Siple transmitter signal and natural VLF chorus observed at ground-based chain stations

near Roberval, Quebec. *J. Geophys. Res.: Space Phys*. 1982, vol. 87, iss. A2, pp. 742–750. DOI: 10.1029/JA087iA02p00742.

Xu T., Rietveld M., Wu J., Ma G., Hu Y., Wu J., Li Q. Polarization analysis of ELF/VLF waves generated by beating of two HF waves in the polar ionosphere. *J. Atmos. Solar-Terr. Phys.* 2019, vol. 196, 105133. DOI: 10.1016/j.jastp.2019.105133.

Yearby K.H., Smith A.J. The polarization of whistlers received on the ground near L=4. *J. Atmos. Terr. Phys.* 1994, vol. 56, pp. 1499–1512. DOI: 10.1016/0021-9169(94)90117-1.

Original Russian version: Nikitenko A.S., Lebed O.M., Larchenko A.V., Fedorenko Yu.V., published in Solnechno-zemnaya fizika. 2026, vol. 12, no. 1, pp. 64–73. DOI: 10.12737/szf-121202608.

How to cite this article

Nikitenko A.S., Lebed O.M., Larchenko A.V., Fedorenko Yu.V. Analyzing events of simultaneous ground-based registration of auroral hiss bursts and riometric absorption increase. *Sol.-Terr. Phys*. 2026, vol. 12, iss. 1, pp. 59–67. DOI: 10.12737/stp-121202608.